



Evaluation of Sea Surface Wind Products from Scatterometer Onboard the Chinese HY-2D Satellite

Sheng Yang^{1,2}, Lu Zhang^{3,*}, Mingsen Lin^{1,2} , Juhong Zou^{1,2} , Bo Mu^{1,2} and Hailong Peng^{1,2}

¹ National Satellite Ocean Application Service, Beijing 100081, China

² Key Laboratory of Space Ocean Remote Sensing and Application, Ministry of Natural Resources, Beijing 100081, China

³ National Marine Environmental Forecasting Center, Beijing 100081, China

* Correspondence: zhanglu@nmefc.cn

Abstract: The Chinese new marine dynamic environment satellite HY-2D was launched on 19 May 2021, carrying a Ku-band scatterometer (named HSCAT-D). In this study, wind products observed by the HSCAT-D were validated by comparing with wind data from the U.S. National Data Buoy Center (NDBC) buoys and European Centre for Medium-Range Weather Forecasts (ECMWF) model. The statistical results show that the HSCAT-D winds have a good agreement with the buoys' wind measurements: in comparison with buoy winds, the wind speed standard deviation (STD) and root-mean-squared errors (RMSE) of direction were 0.78 m/s and 14.10°, respectively. Other scatterometers' wind data are also employed for comparisons, including the HY-2B scatterometer (HSCAT-B), HY-2C scatterometer (HSCAT-C), and MetOp-B scatterometer (ASCAT-B) winds. The statistical results indicate that errors for HSCAT-D winds are smaller than HSCAT-C but a little bit larger than HSCAT-B. The spectral analysis shows that the HSCAT-D wind products contain less small-scale information than ASCAT-B. Moreover, the Extended Triple Collocation (ETC) results show that the HSCAT-D wind product is of good quality and well-calibrated. We believe that the HSCAT-D wind products will be helpful for the scientific community, as shown by the encouraging validation results.

Keywords: ocean surface wind; scatterometer; validation



Citation: Yang, S.; Zhang, L.; Lin, M.; Zou, J.; Mu, B.; Peng, H. Evaluation of Sea Surface Wind Products from Scatterometer Onboard the Chinese HY-2D Satellite. *Remote Sens.* **2023**, *15*, 852. <https://doi.org/10.3390/rs15030852>

Academic Editor: Vladimir N. Kudryavtsev

Received: 16 December 2022

Revised: 20 January 2023

Accepted: 1 February 2023

Published: 3 February 2023



Copyright: © 2023 by the authors. Licensee MDPI, Basel, Switzerland. This article is an open access article distributed under the terms and conditions of the Creative Commons Attribution (CC BY) license (<https://creativecommons.org/licenses/by/4.0/>).

1. Introduction

The Chinese new HY-2D satellite was launched on 19 May 2021, carrying the scatterometer named HSCAT-D with Ku-band. After the HY-2D launch, a three-star observation network with an on-orbit HY-2B and HY-2C was built, forming the HY-2 series spaceborne scatterometer constellation. In this way, an all-weather, all-day, high-frequency, medium-, and large-scale global monitoring system of the ocean dynamic environment has been achieved. The constellation will provide precise ocean dynamic environmental information for the warning and forecasting of marine disasters, continuous development, and utilization of marine resources, effective combat against global climate change, etc.

The HSCAT-D scatterometer is intended for monitoring sea surface wind. It is similar to the former scatterometer instruments HSCAT-B and HSCAT-C, which were carried by HY-2B and HY-2C. However, the satellite HY-2D flies in a different orbit compared to HY-2B. The HY-2B spacecraft operates at an inclination of 99.3°, leading the local equator crossing time to be about 6:00. Nevertheless, the HY-2D's non-sun-synchronous orbit and 66.0° inclination cause its equator crossing time to shift each day. The HSCAT-D winds could be complementary to the wind retrieved by its predecessors, which improves the inter-calibration and wind processing of all China scatterometer systems. The Meteorological operational satellite-B (MetOp-B) is a polar-orbiting satellite carrying a C-band scatterometer named ASCAT-B. Both the European Space Agency (ESA) and the European

Organisation for the Exploitation of Meteorological Satellites (EUMETSAT) are collaborating in its development. The abundant scatterometer winds will also promote the development of nowcasting applications and other scientific studies [1,2].

Several previous studies have demonstrated that comparisons between scatterometer-retrieved winds and other winds are an effective way to evaluate the quality of scatterometer winds [3,4]. For instance, the wind data measured by the first conical scanning scatterometer QuikSCAT/SeaWinds are validated by comparison with the wind from the ocean buoy, and the results show good consistency [5,6]. Similar validation studies of the HY-2 series scatterometers have been carried out by other researchers [7–11]. However, HSCAT-D wind validation has not been addressed so far in previous publications to our knowledge. Examining the precision of the HSCAT-D scatterometer wind products is the main goal of this study: the HSCAT-D winds are validated by collocated datasets from buoys operated by NDBC. The ECMWF winds are also compared to the HSCAT-D winds for the overall comparison, and systematic errors of pencil-beam rotating scanning scatterometer are analyzed.

Analyzing the wind components' spectra to investigate noise, and by integrating the difference between the spectra from the scatterometer and model winds, one may calculate the relative quantity of small-scale information. The correlated error is obtained in this study [11,12].

Previous studies suggest that data representing “true” winds usually contain validation results, calibration errors, and measurement bias [13]. Assuming that a given triplet of measurement collocation has been linearly calibrated, the measurement bias and related calibration coefficients can be computed simultaneously. Therefore, an Extended Triple Collocation (ETC) method was conducted to evaluate the buoy, ECMWF, and scatterometer winds' error. The ETC approach uses the same assumptions as Triple Collocation (TC): when using the estimated buoy observation error, it can give the low-resolution NWP model, the medium-resolution scatterometer, or the measurement error from the high-resolution buoy. In contrast, the difference between ETC and TC is that the correlation coefficients of the measuring system with regard to the “true” values were derived as an extra performance parameter [14,15].

Rainfall will increase the backscattering coefficient at medium- and low wind speeds, while it decreases and dominates the attenuation effect at high wind conditions. The sensitivity to precipitation of the Ku-band scatterometer is an issue that affects it severely when there is a complex sea surface state. Therefore, the removal of data contaminated by rainfall is of great significance for the successful evaluation of wind data from HSCAT scatterometers. If the KNMI QC (the Royal Netherlands Meteorological Institute Quality Control) flag is present in a wind vector cell, the WVC is not useful for many geophysical reasons, such as precipitation and complicated sea-state, and should be abandoned in the calculation of the ambiguity removal step to avoid causing a large inversion residual [16]. Here, we rejected the KNMI QC-flagged winds.

The scatterometer data, ECMWF model data, NDBC buoy data, and collocated datasets are outlined in Section 2. Section 3 summarizes the statistical results and analyzes the quality of HSCAT-D wind products. Section 4 discusses the related results. Conclusions are presented in Section 5.

2. Data and Methods

2.1. ECMWF NWP Data

The ECMWF winds are required as the background model winds in the ambiguity removal processing step; thus, the HSCAT and ASCAT wind files already contain the ECMWF forecast data, which were interpolated to scatterometer wind products spatially and temporally. The wind product validation for the HSCAT and ASCAT in this study employed the stored background winds. There are three forms of wind data: real winds, equivalent neutral winds, and stress-equivalent (SE) winds [17]. The wind retrieved by the scatterometer is the stress equivalent wind at a height of 10 m from the sea surface.

The Royal Netherlands Meteorological Institute (KNMI) currently processes scatterometer wind data using ECMWF stress-equivalent winds as background wind, whereas NSOAS processes scatterometer data using actual winds.

2.2. Buoy Winds

We collocated wind measurements from Standard Meteorological data of 56 NDBC buoys operated by the NDBC during the same period of HSCAT-D winds. To avoid the impact of land pollution on the accuracy of winds measured by the HSCAT scatterometer, only buoys with an offshore distance greater than 50 km were used. The geographical locations of the collocated buoys in this work are presented in Figure 1.

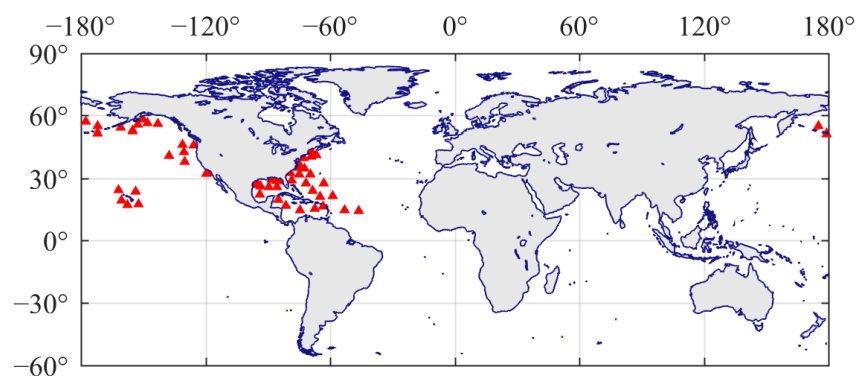


Figure 1. Locations of the collocated buoys.

The buoys obtain the actual wind at its anemometer height, which is between 3.5 m and 5 m above sea level, at 10-min intervals. Direct comparison between uncorrected reference buoy winds and scatterometer-derived winds can cause systematic and random errors. Scatterometer winds have been demonstrated to be more consistent with equivalent-neutral winds and are better for comparison [17]. Thus, we converted the buoy winds to equivalent neutral winds at a height of 10 m above the sea surface using the method of Liu and Tang [18].

2.3. HSCAT Scatterometer Wind Products

This study used HSCAT-D, HSCAT-B, and HSCAT-C operational 25 km swath grid L2B products, which require significant wind retrieval processing (the Pencil beam Wind Processor, PenWP) before being distributed by the ground-based application systems of the National Satellite Ocean Application Service (NSOAS) [19]. These improved wind-derived products were manipulated using the multiple solution scheme (MSS) for wind retrieval with the NSCAT-4 geophysical model function, in conjunction with the two-dimensional variational ambiguity removal (2DVAR) approach to remove ambiguity. The ECMWF forecast real wind data were used for background winds. Previous research has shown that the multiple solution scheme (MSS) method in conjunction with the 2-DVAR may generate better wind products for rotating-beam scatterometers [20,21]. Table 1 shows the detailed parameters of the HSCAT-D scatterometer and other scatterometers. The HSCAT-B, HSCAT-C, and HSCAT-D scatterometer wind products are publicly distributed to users and can be obtained through the website (<https://osdds.nsoas.org.cn/>, accessed on 1 December 2022).

2.4. ASCAT-B Scatterometer Wind Products

The ASCAT-B L2 wind products on the 25 km resolution used in this study are processed by the Royal Netherlands Meteorological Institute (KNMI) within the framework of the Ocean and Sea Ice Satellite Application Facility (OSI SAF), using the CMOD7 GMF [22]. Using the 2-DVAR method in the ASCAT wind retrieval process, the “best” wind was

selected after using the maximum likelihood estimation (MLE) method. The method was based on the Bayesian probability theorem [10].

Table 1. Parameters of HSCAT-B, HSCAT-C, HSCAT-D, and ASCAT-B.

	HSCAT-B	HSCAT-C	HSCAT-D	ASCAT-B
Frequency	13.256 GHz	13.256 GHz	13.256 GHz	5.255 GHz
Polarization mode	HH + VV	HH + VV	HH + VV	VV
Spatial resolution	25 km × 25 km			
Swath width	1350 km(H)/1700 km(V)	1350 km(H)/1700 km(V)	1350 km(H)/1700 km(V)	500 km
Incidence angles	48°(V)/41°(H)	48°(V)/41°(H)	48°(V)/41°(H)	25°–65°
Antenna	Rotating pencil beam	Rotating pencil beam	Rotating pencil beam	Fan beam
Wind speed precision	±2 m/s or 10% (2~24 m/s)	±2 m/s or 10% (2~24 m/s)	±2 m/s or 10% (2~24 m/s)	±2 m/s or 10% (4~24 m/s)
Wind direction precision	±20°	±20°	±20°	±20°

2.5. Collocated Datasets

In this paper, 16 months (from 1 June 2021 to 31 October 2022) of the HSCAT-D, HSCAT-B, HSCAT-C, and ASCAT-B datasets were matched with ECMWF and buoy data and assessed. The scatterometer wind vector cells closest to the buoy locations in space and the buoy data closest to the scatterometer observations in time were chosen. The spatial interval and time difference of scatterometer and buoy observations were set within $25/\sqrt{2}$ km and 30 min, respectively. In addition, the scatterometer winds were compared with their background ECMWF winds; that is, ECMWF real winds for HSCAT and ECMWF stress-equivalent winds for ASCAT-B.

3. Results and Analysis

Only winds larger than 3 m/s were selected for accuracy analysis. The comparison statistics were further refined by eliminating the KNMI QC flagged data. The breakpoint between 0° and 360° will cause the statistical results of wind direction to deviate from the actual situation. For example, for the wind direction of 350° and 10°, the difference between the direct subtraction values is 340°, while the actual difference is only 20°. Such cross-360° wind direction data were converted using the method given by other researchers [8]. However, the wind direction in the scatter plot was not converted to reveal the distribution characteristics of the wind direction.

3.1. Comparison with Buoy Winds

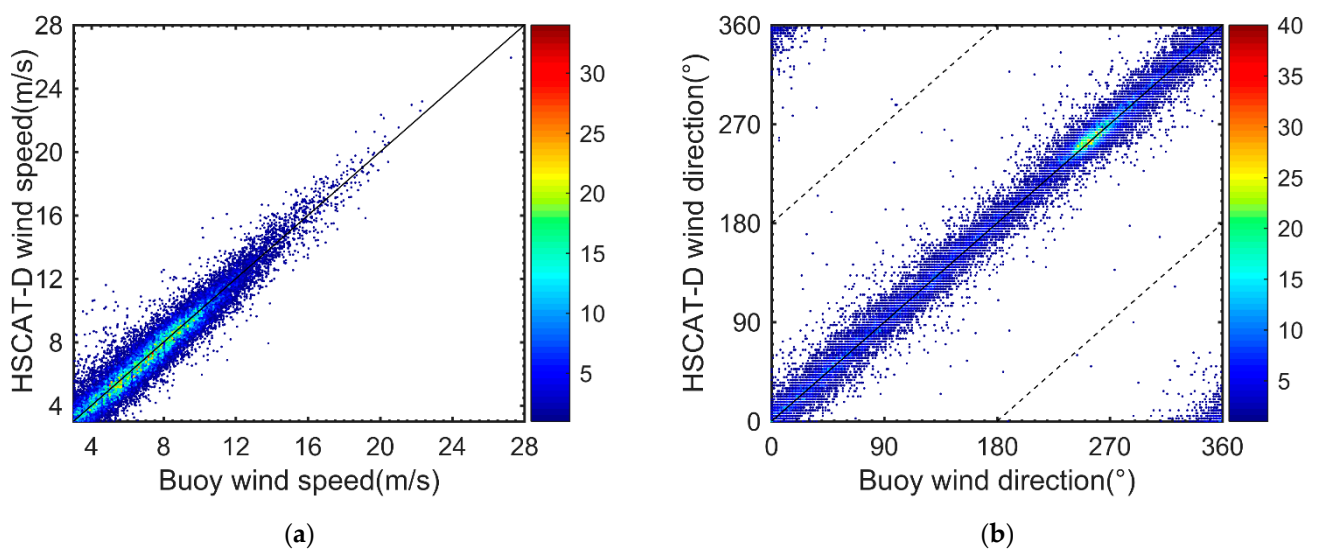
The full sixteen months scatterometer–buoy collocated datasets are matched and compared below. Bad scatterometer data was rejected using the KNMI QC flag described above. Since the HSCAT-D scatterometer has the same swath width as the other HSCAT scatterometers, which operates in the same 66° inclined orbit as the HSCAT-C scatterometer, it provides relatively increased numbers of collocated scatterometer–buoy matchups than HSCAT-B (99.34° inclination orbit) in 74° N and 74° S latitudes where all NDBC buoys are located. The ASCAT-B has a narrower swath width than HSCAT, and the MetOp-B satellite uses a polar orbit, and therefore provides the lowest number of matchups.

The statistical results summarized in Table 2 demonstrate that wind bias between HSCAT-D and buoys showed very similar statistics with other scatterometers. The wind speed bias of HSCAT-D was slightly negative, indicating that scatterometer-derived wind speed was slightly underestimated. The STDs of the v component and u component were also compared: the difference among other scatterometers was less than 0.09 m/s, and −0.01 m/s for HSCAT-D. For the wind direction, the RMSE of the HSCAT-D scatterometer was 14.10°, which was slightly higher than HSCAT-B but lower than HSCAT-C and ASCAT-B. All of the results are in a small deviation and comparable.

Table 2. Statistics of comparisons between scatterometer wind and buoy wind.

Name	Number	Speed		U		V		Direction
		Bias (m/s)	STD (m/s)	Bias (m/s)	STD (m/s)	Bias (m/s)	STD (m/s)	RMSE (°)
HSCAT-D	23,229	−0.03	0.78	−0.01	1.18	−0.01	1.23	14.10
HSCAT-B	20,696	−0.07	0.77	0.04	1.18	−0.03	1.18	13.92
HSCAT-C	23,979	−0.04	0.81	0.03	1.26	−0.04	1.28	15.10
ASCAT-B	14,573	−0.01	0.77	0.04	1.08	0.09	1.24	14.97

Figure 2 shows the scatterplots of wind derived from HSCAT-D versus NDBC buoy wind. The direction scatter plot reveals the characteristics of the wind direction distribution: there are sporadic sample distributions in the upper left and lower right corners, which can be attributed to the cross-360° wind direction problem.

**Figure 2.** Scatterplots of wind speed (a) and direction (b) derived from HSCAT-D versus NDBC buoy winds.

The scatterometer's wind speed bias and wind direction bias monthly averages for the time from June 2021 to October 2022 are displayed in Figure 3. The wind speed bias of HSCAT-D was approximately -0.3 m/s to 0.3 m/s. What can be seen in Figure 3 is the clear annual oscillation in the wind speed bias. The cause is not fully understood; we attribute it to seasonal wind speed and sea surface temperature (SST) distribution in the Northern Hemisphere, seasonally dependent buoy measurement error, and the use of NSCAT-4 GMF without SST correction. The wind direction bias, in contrast, did not exhibit comparable yearly fluctuation, since the accuracy of the wind direction is mostly dependent on the wind speed. Noteworthy is the fact that the wind speed deviation of HSCAT-D in December 2021 showed a notable decrease, which could be due to calibration and processing settings. The previous study indicated that 0.25 m/s wind speed bias may be caused by the 0.2 dB calibration error [23]. The long-term trend of the HSCAT-D wind bias still needs further investigation.

3.2. Comparison with ECMWF Model Winds

The overall statistical results are reported in Table 3. Screened by the KNMI QC discrimination, the rejected ratios of HSCAT-D, HSCAT-B, HSCAT-C, and ASCAT-B were 7.7%, 6.3%, 6.5%, and 1.0%, respectively. For ASCAT, the QC-rejected ratio was smaller because the influence of rainfall on C-band observations was less than that of the Ku-band. The ECMWF data and HSCAT-D wind speed and direction agreed well, i.e., the STDs of wind speed differences was 1.15 m/s. In contrast to the scatterometer–buoy comparison

result, the wind speed biases between HSCAT and ECMWF were all slightly positive, and the mean value of HSCAT-D was 0.09 m/s. This may be due to HSCAT winds being compared to ECMWF real winds, which are on average 0.2 m/s lower than ECMWF stress-equivalent winds [17].

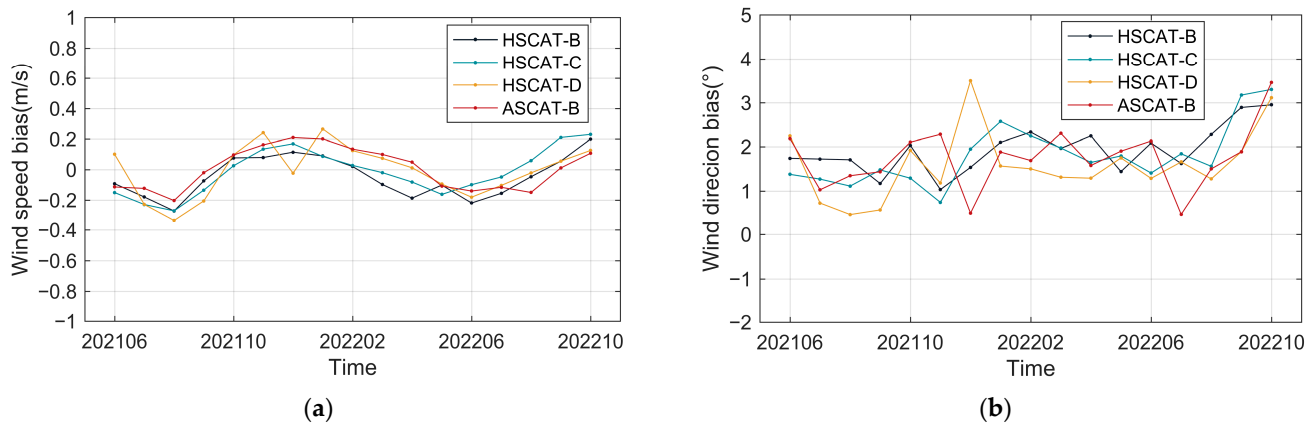


Figure 3. The bias of scatterometer wind speed (a) and direction (b) versus buoys from June 2021 to October 2022.

Table 3. Statistics of comparisons between scatterometer wind and ECMWF wind.

Name	QC	Speed		U		V		Direction
		Bias (m/s)	STD (m/s)	Bias (m/s)	STD (m/s)	Bias (m/s)	STD (m/s)	RMSE (°)
HSCAT-D	7.7%	0.09	1.15	−0.18	1.25	0.00	1.25	12.79
HSCAT-B	6.3%	0.06	1.14	−0.10	1.26	0.06	1.21	12.69
HSCAT-C	6.5%	0.07	1.14	−0.16	1.29	0.00	1.27	13.51
ASCAT-B	1.0%	0.04	1.04	−0.06	1.28	−0.09	1.37	14.27

Figure 4a shows the collocated data of wind speed between scatterometer–ECMWF, which were concentrated in the range of 2 m/s–16 m/s. When the wind speed exceeded 18 m/s, the number of matchups was scarce. Figure 4b depicts the probability distribution functions (PDFs) of wind speed from each scatterometer. The wind speed residuals were almost zero, indicating that none of the scatterometers depend systematically on the ECMWF wind speed in the range of 3 to 30 m/s.

Two-dimensional scatterplots of the HSCAT-D winds versus ECMWF winds are illustrated in Figure 5. The left panel corresponds to wind speed and the right panel to wind direction. Only winds larger than 3 m/s were used to calculate.

Figure 6a displays the wind speed bias as a function of average wind speed between scatterometers and model winds. The HSCAT-D, HSCAT-B, and HSCAT-C showed similar wind bias characteristics. However, it is evident that all scatterometers had a positive wind speed bias with regard to the ECMWF for winds greater than 15 m/s, particularly when wind speed exceeded 20 m/s, which reveals that HSCAT-derived wind speed was slightly underestimated in the high wind speed range (>15 m/s). The high-speed correction of NSCAT-4 GMF was obtained by comparing scatterometer wind speed with buoy and model winds. Due to the scarcity of reliable in situ wind speed observations, it should be noted that high wind speed calibration is also questionable. Compared with the scatterometer, the NWP model has a coarser resolution and contains less small-scale detail information. Hence, scatterometer winds might display a different wind climate than ECMWF winds for strong winds. The other reason could be related to the non-linearity in the instrument backscatter calibration or the small number of samplings, which need further investigation. For ASCAT-B, Figure 6 shows that it had a smaller deviation than HSCAT in the middle- and high-wind-speed range; this might be caused by the utilization of stress-equivalent wind as background wind.

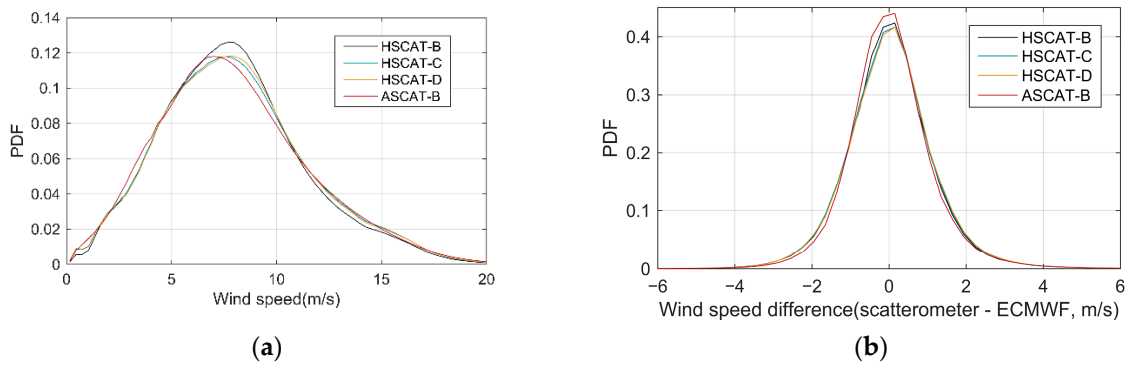


Figure 4. Wind speed probability distribution functions of each scatterometer (a) and wind speed deviation PDFs of scattermeters vs. ECMWF data (b).

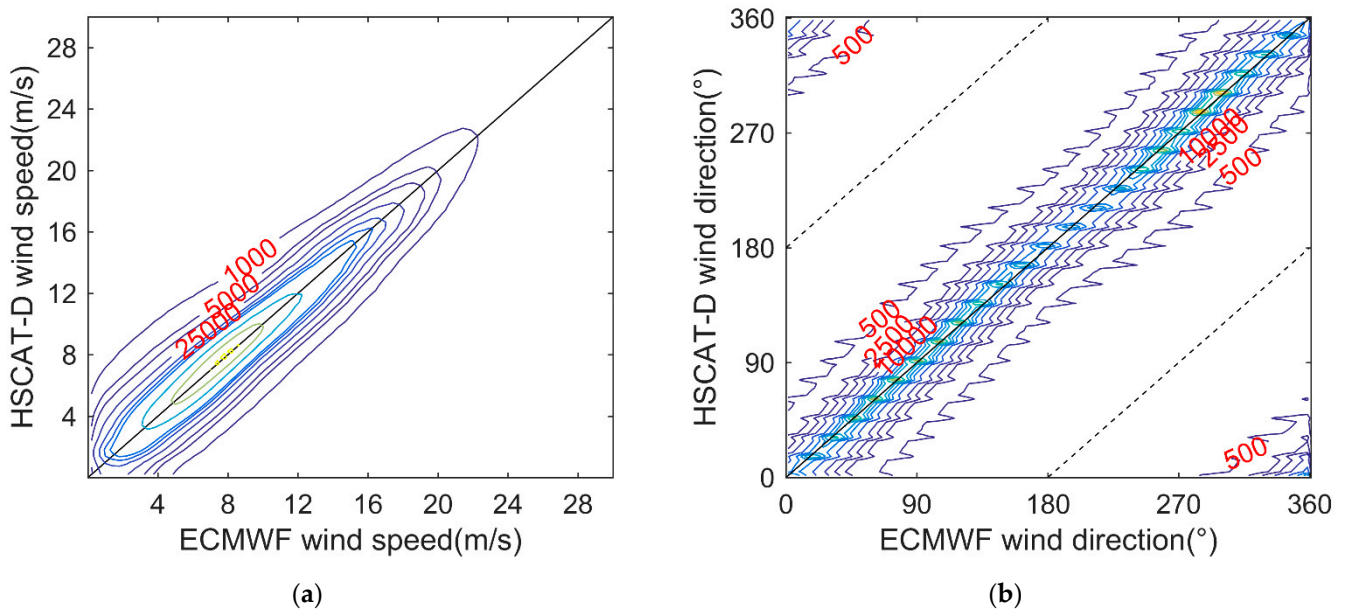


Figure 5. Scatterplots of wind speed (a) and direction (b) derived from HSCAT-D versus ECMWF winds.

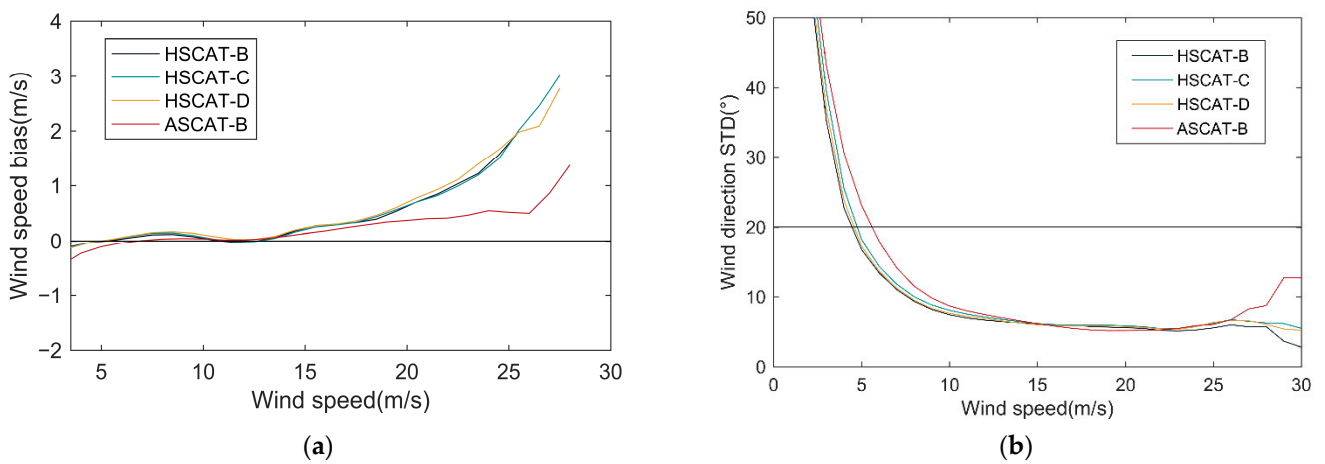


Figure 6. Wind speed bias as a function of average wind speed between scattermeters and model winds (a) and the standard deviation of wind direction difference between scattermeters and ECMWF as a function of average wind speed (b).

The wind direction error STD increased rapidly at low wind speed, corresponding to the results shown in Figure 6b. When the wind speed was below 5 m/s, the STD of the wind direction retrieval was larger than 20° . The standard deviation of ASCAT-B was slightly higher than the other HSCAT when wind speed was less than 14 m/s. In general, when wind speed was higher than 7 m/s, all standard deviation of HSCAT wind direction retrieval remained less than 10° .

All of the HSCAT scattermeters carry a rotating dish antenna with two pencil beams that sweep in a circular pattern, resulting in systematic cross-track variability in the accuracy of the wind retrieval. In terms of wind speed standard deviation, Figure 7a compares the wind differences between HSCAT and ECMWF as a function of the cross-track WVC index. When wind vector cells are located in the nadir swath (Cell Number in [20,60]), the wind speed difference STDs of the HSCAT-D are less than 1.2 m/s. For the outer swath (Cell Number in [1,10] and [69,76]), where only vertically polarized beams can illuminate, the standard deviations increased rapidly and the accuracy of wind products degraded in the edge swath. For the wind direction, noticeable differences were also found in the middle and edge of the swaths. The overall cross-track wind direction difference STDs of HSCAT-D and HSCAT-B were less than 4° . However, the wind direction difference STD of HSCAT-C was slightly larger (by approximately 1°).

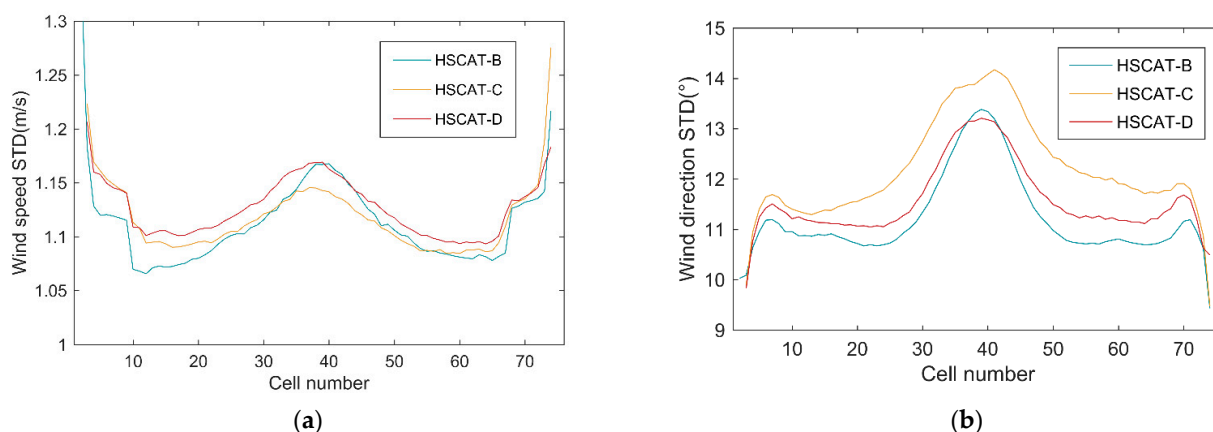


Figure 7. Cross-track variations in comparisons between scatterometer winds and ECMWF winds: (a) STD of wind speed differences, and (b) STD of wind direction differences.

3.3. Spectral Analysis

Figure 8 shows the scatterometer and ECMWF wind spectra for the *u* and *v* wind components: spectra of the HSCAT-B (red), HSCAT-C (green), HSCAT-D (black), and ASCAT-B (pink) wind products for (left) the *u*-component and (right) the *v*-component. The blue curve is the spectrum for the ECMWF background real wind.

The spectral content of HSCAT-D was lower than ASCAT-B, which means that HSCAT-D wind products contain less detailed information than ASCAT-B. This is due to the 2DVAR after MSS was applied in HSCAT. In addition, compared to the ASCAT-B spectra, the HSCAT spectra were more similar to the ECMWF model spectra, demonstrating that HSCAT has a higher agreement with the ECMWF and less agreement with the buoys.

3.4. Extended Triple Collocation Results

McColl originally proposed the Extended Triple Collocation (ETC) method in 2014, and it was used to calculate the measuring system performance metric: the error standard deviation, the correlation coefficient, and the calibration coefficient of each measurement system concerning the “true” wind [15].

Table 4 shows the standard deviations of errors in the *u* and *v* wind components obtained from the extended triple collocation of the scatterometer with buoy and ECMWF winds, and the correlation coefficients are listed in Table 5. The estimation results show that the STDs were small and the correlation coefficients all approached 1. For instance, the

HSCAT-D scatterometer’s wind component error STD was around 0.6 m/s, as compared to the unknown true winds. The errors for HSCAT-D were slightly less than HSCAT-C but somewhat larger than the corresponding errors for HSCAT-B and ASCAT-B.

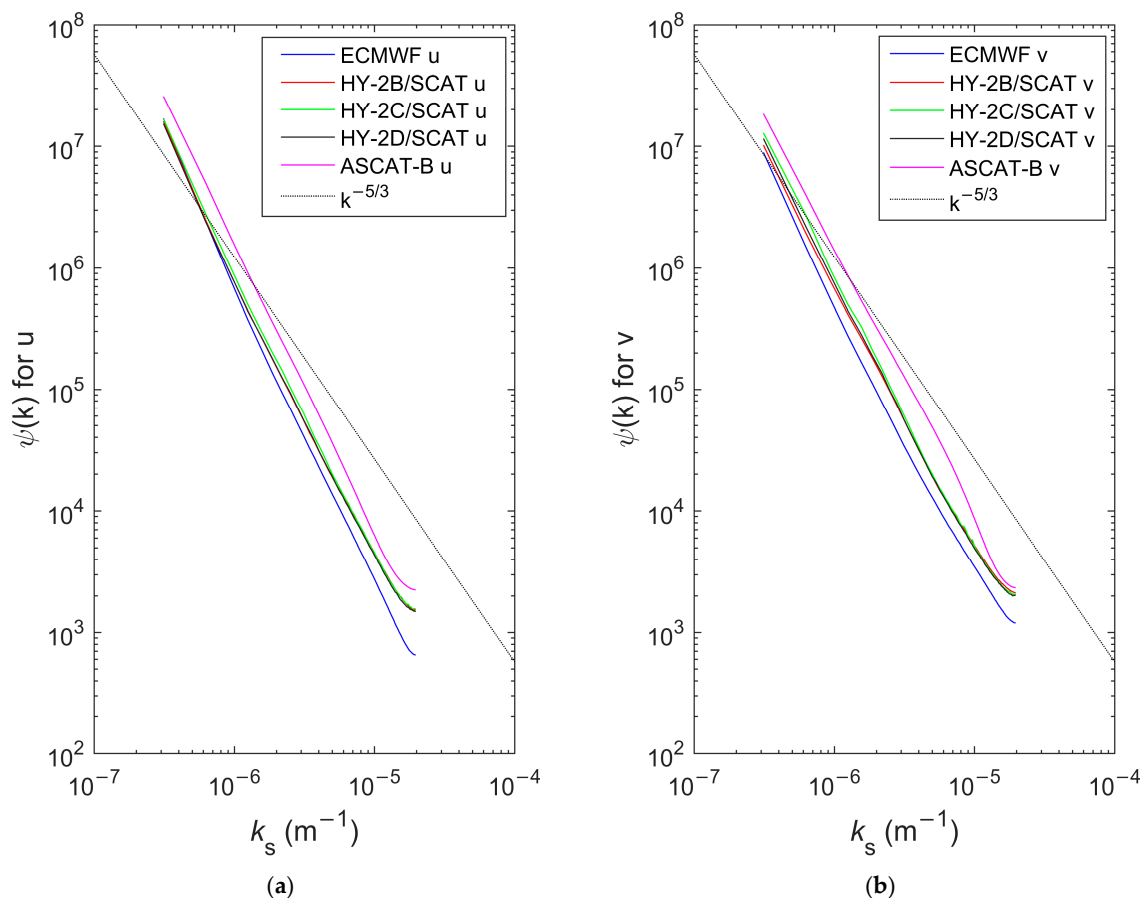


Figure 8. Spectra of the HSCAT-B (red), HSCAT-C (green), HSCAT-D (black), and ASCAT-B (pink) wind and ECMWF background real wind (blue) for (a) u-component and (b) v-component.

Table 4. Standard deviations of errors in the u and v wind components obtained from the ETC of the scatterometer with buoy and ECMWF winds.

NAME	Scatterometer		Buoy		ECMWF	
	ϵ_u (m/s)	ϵ_v (m/s)	ϵ_u (m/s)	ϵ_v (m/s)	ϵ_u (m/s)	ϵ_v (m/s)
HSCAT-B	0.60	0.46	1.02	1.08	0.98	1.00
HSCAT-C	0.71	0.63	1.04	1.11	0.97	0.96
HSCAT-D	0.61	0.57	1.00	1.09	0.97	0.96
ASCAT-B	0.39	0.54	1.00	1.11	1.16	1.20

Table 5. The correlation coefficient in u and v wind components from the ETC of the scatterometer with buoy and ECMWF winds.

NAME	Scatterometer		Buoy		ECMWF	
	ρ_u	ρ_v	ρ_u	ρ_v	ρ_u	ρ_v
HSCAT-B	0.995	0.996	0.985	0.978	0.987	0.981
HSCAT-C	0.993	0.993	0.985	0.977	0.988	0.982
HSCAT-D	0.995	0.994	0.986	0.978	0.987	0.982
ASCAT-B	0.998	0.995	0.986	0.978	0.982	0.973

We may also ascertain the scatterometer winds' calibration coefficients from the ETC analysis. According to the formula $r = a \times w + b$, the calibration coefficients connect the measured scatterometer wind w to the 'real' wind r . U and v wind components are processed individually. Moreover, $a > 1$ and $a < 1$, respectively, indicate that the scatterometer wind is underestimated or overestimated compared with the true wind. Table 6 shows the calibration coefficients for u and v wind components. We can see that all a values are close to 1, and the b values are close to 0. The lower values for ASCAT-B are likely due to nonlinearities in the wind inversion. In summary, the result of ETC shows the good quality of the HSCAT-D wind products.

Table 6. Calibration coefficients for u and v wind components from the ETC of the scatterometer with buoy and ECMWF winds.

Name	a_u	a_v	b_u (m/s)	b_v (m/s)
HSCAT-B	1.003	0.986	0.057	0.104
HSCAT-C	0.994	0.987	0.064	0.096
HSCAT-D	0.993	0.984	0.091	0.061
ASCAT-B	0.983	0.981	0.013	−0.035

4. Discussion

4.1. Comparison with Other Wind Sources

The statistical results indicate that errors for HSCAT-D winds were smaller than HSCAT-C, but slightly larger than HSCAT-B, compared with buoys. The HSCAT-C wind direction showed worse agreement with buoy winds. Thus, further calibration of HSCAT-D and HSCAT-C σ_0 measurements and wind products is still suggested for future study. A clear annual oscillation was found for all scatterometer wind speed biases; these biases are probably due to differences in wind speed distribution and sea surface temperature (SST) distribution in the Northern Hemisphere caused by seasonal weather changes. These differences lead to changes in the spatial representation errors associated with scatterometer wind validation and thus in the difference statistics. In addition, seasonally dependent buoy measurement error and the use of NSCAT-4 GMF without SST correction may also be responsible for this phenomenon (previous studies have shown that SST may affect the Ku-band sea surface backscatter coefficient, resulting in the influence of Ku-band scatterometer wind speed retrieval) [24]. We also performed a comparison of scatterometer winds with ECMWF winds. For high wind speeds, all scatterometer winds showed significant deviation in wind speed biases because of the lack of consistent in situ measurements. Therefore, the NSCAT-4 geophysical model function (GMF) needs further improvement. The accuracy of HSCAT winds varied across the swath, and it was relatively poor in the middle and edge regions of the swath.

4.2. Discussion of Spectral and ETC Results

The spectra of HSCAT-B, HSCAT-C, and HSCAT-D are quite comparable due to using the same payload and processing technique. On the other hand, the spectral content of HSCAT-D is lower than ASCAT-B, which means HSCAT-D wind products contain less detailed information than ASCAT-B. This is due to the 2DVAR after MSS applied in HSCAT decreasing noise at the cost of some detailed information loss by geographically filtering the solutions over a large number of nearby WVCs (such an MSS method basically suppresses the multiple ambiguous solutions by spatial filtering the solutions on adjacent WVCs and reduces the wind direction ambiguity produced by the pencil beam scatterometer) [21]. Data sampling may also be a factor because the spectra were collected at different times and various places throughout the global ocean. In addition, compared to the ASCAT-B spectra, the HSCAT spectra were more similar to the ECMWF model spectra, demonstrating that HSCAT had a higher agreement with the ECMWF and less agreement with the buoys. Moreover, the scatterometer and ECMWF spectra were quite similar for large spatial scales, but for small spatial scales, the ECMWF spectra dropped significantly from the HSCAT

spectra. This is due to the ECMWF model cutoff at small scales suppressing indeterminate small-scale structures in a useful way and avoiding their unfavorable upscale expansion, which would otherwise degrade the accuracy of medium-range forecasts [12].

For the ETC results, the HSCAT-D scatterometer's wind component error STD was around 0.6 m/s and the correlation coefficient almost approached 1, as compared to the unknown true winds. Moreover, we further evaluated the calibration coefficients among triplets and found that the trends and deviations of all triplet data were close to the theoretical optimal values.

5. Conclusions

The wind product quality of the Chinese new Ku-band rotating-beam scatterometer HSCAT-D was examined by comparing with NDBC buoys and ECMWF model data over the period from June 2021 to October 2022. Its older brothers' wind data, including HSCAT-B and HSCAT-C, and ASCAT-B wind produced by KNMI, were also validated. The conclusion is as follows:

Comparison results with buoys show that all scatterometers have a small deviation from buoy and ECMWF winds. The HSCAT-D wind speed STD and RMSE of direction were 0.78 m/s and 14.10° , compared with NDBC buoy winds. However, errors for HSCAT-D winds were smaller than HSCAT-C but slightly larger than HSCAT-B; thus, further calibration of HSCAT-D and HSCAT-C σ_0 measurements and wind products is still suggested for future study. For the spectral analysis, the HSCAT-D wind products contained less small-scale information than ASCAT-B, and had more consistency with the ECMWF model and less consistency with the NDBC buoys. The result of ETC shows the good quality of the HSCAT-D wind products. However, the small overestimation of the wind components by HSCAT series scatterometers is unclear and is subject to future research.

In general, the HSCAT-D scatterometer meets the design and mission requirements (<2 m/s and 20°). The HSCAT-D wind products show good quality and perform consistently with the buoy and ECMWF winds. A better understanding of the error characteristics of HSCAT-D would greatly contribute to applications and scientific research.

Author Contributions: Validation, B.M.; Resources, H.P.; Data curation, J.Z.; Writing—original draft, S.Y.; Writing—review and editing, S.Y. and L.Z.; Project administration, M.L. All authors have read and agreed to the published version of the manuscript.

Funding: This research was funded by National Key R&D Program of China, grant number 2021YFB3900400.

Data Availability Statement: The NSOAS HSCAT L2B data products are available at <https://osdds.nsoas.org.cn/> (accessed on 1 December 2022).

Conflicts of Interest: The authors declare no conflict of interest.

References

1. Stoffelen, A.; van Beukering, P. The impact of improved scatterometer winds on HIRLAM analyses and forecasts. *BCRS Study Contract* **1997**, 1.
2. Isaksen, L.; Stoffelen, A. ERS scatterometer wind data impact on ECMWF's tropical cyclone forecasts. *IEEE Trans. Geosci. Remote Sens.* **2000**, *38*, 1885–1892. [[CrossRef](#)]
3. Freilich, M.; Dunbar, R. The accuracy of the NSCAT 1 vector winds comparisons with national data buoy center buoys. *J. Geophys. Res.* **1999**, *104*, 11231–11246. [[CrossRef](#)]
4. Bentamy, A.; Croize-Fillon, D.; Perigaud, C. Characterization of ASCAT measurements based on buoy and QuikSCAT wind vector observations. *Ocean. Sci.* **2008**, *4*, 265–274. [[CrossRef](#)]
5. Ebuchi, N.; Graber, H.; Caruso, M. Evaluation of wind vectors observed by QuikSCAT/SeaWinds using ocean buoy data. *J. Atmos. Ocean. Technol.* **2002**, *19*, 2049–2062. [[CrossRef](#)]
6. Chelton, D.; Freilich, M. Scatterometer-based assessment of 10 m wind analyses from the operational ECMWF and ECMWF numerical weather prediction models. *Mon. Weather. Rev.* **2005**, *133*, 409–429. [[CrossRef](#)]
7. Wang, H.; Zhu, J.; Lin, M.; Huang, X.; Zhao, Y.; Chen, C.; Zhang, Y.; Peng, H. First six months quality assessment of HY-2A SCAT wind products using in situ measurements. *Acta Oceanol. Sin.* **2013**, *32*, 27–33. [[CrossRef](#)]

8. Mu, B.; Lin, M.; Peng, H.; Song, Q.; Zhou, W. Validation of wind vectors retrieved by the HY-2 microwave scatterometer using ECMWF model data. *Eng. Sci.* **2014**, *16*, 39–45.
9. Zhu, J.; Dong, X.; Yun, R. Calibration and validation of the HY-2 scatterometer backscatter measurements over ocean. In Proceedings of the 2014 IEEE Geoscience and Remote Sensing Symposium, Quebec City, QC, Canada, 13–18 July 2014; pp. 4382–4385.
10. Wang, Z.; Stoffelen, A.; Zou, J.; Lin, W.; Verhoef, A.; Zhang, Y.; He, Y.; Lin, M. Validation of New Sea Surface Wind Products from Scatterometers Onboard the HY-2B and MetOp-C Satellites. *IEEE Trans. Geosci. Remote Sens.* **2020**, *58*, 4387–4394. [[CrossRef](#)]
11. Wang, Z.; Zou, J.; Stoffelen, A.; Lin, W.; Verhoef, A.; Li, X.; He, Y.; Zhang, Y.; Lin, M. Scatterometer Sea Surface Wind Product Validation for HY-2C. *IEEE J. Sel. Top. Appl. Earth Obs. Remote Sens.* **2021**, *14*, 6156–6164. [[CrossRef](#)]
12. Vogelzang, J.; Stoffelen, A.; Verhoef, A.; Figurea-Saldaña, J. On the quality of high-resolution scatterometer winds. *J. Geophys. Res. Oceans* **2011**, *116*, 1–14. [[CrossRef](#)]
13. Chakraborty, A.; Kumar, R.; Stoffelen, A. Validation of ocean surface winds from the OCEANSAT-2 scatterometer using triple collocation. *Remote Sens. Lett.* **2013**, *4*, 85–94. [[CrossRef](#)]
14. Stoffelen, A. Toward the true near-surface wind speed: Error modeling and calibration using triple collocation. *J. Geophys. Res.* **1998**, *103*, 7755–7766. [[CrossRef](#)]
15. McColl, K.A.; Vogelzang, J.; Konings, A.G.; Entekhabi, D.; Piles, M.; Stoffelen, A. Extended triple collocation: Estimating errors and correlation coefficients with respect to an unknown target. *Geophys. Res. Lett.* **2014**, *41*, 6229–6236. [[CrossRef](#)]
16. Verhoef, A.; Stoffelen, A. *Quality Control of Ku-Band Scatterometer Winds*; SAF/OSI/CDOP2/KNMI/TEC/RP/194; OSI SAF: De Bilt, The Netherlands, 2012.
17. de Kloe, J.; Stoffelen, A.; Verhoef, A. Improved Use of Scatterometer Measurements by Using Stress-Equivalent Reference Winds. *IEEE J. Sel. Top. Appl. Earth Obs. Remote Sens.* **2017**, *10*, 2340–2347. [[CrossRef](#)]
18. Liu, W.; Tang, W. *Equivalent Neutral Wind*; California Institute of Technology: Pasadena, CA, USA, 1996.
19. National Satellite Ocean Application Service (NSOAS). HY-2B Scatterometer Wind Product User Manual, Version 1.1, 2018, NSOAS. Available online: <https://osdds.nsoas.org.cn/> (accessed on 1 December 2022).
20. Stoffelen, A.; Portabella, M. On Bayesian scatterometer wind inversion. *IEEE Trans. Geosci. Remote Sens.* **2006**, *44*, 1523–1533. [[CrossRef](#)]
21. Wang, Z.; Zhao, C.; Zou, J.; Xie, X.; Zhang, Y.; Lin, M. An improved wind retrieval algorithm for the HY-2A scatterometer. *Chin. J. Oceanol. Limnol.* **2015**, *33*, 1201–1209. [[CrossRef](#)]
22. OSI SAF/EARS Winds Team. ASCAT Wind Product User Manual. SAF/OSI/CDOP/KNMI/TEC/MA/126, Version 1.17, OSI SAF. 2021. Available online: https://scatterometer.knmi.nl/publications/pdf/ASCAT_Product_Manual.pdf (accessed on 1 December 2021).
23. Stoffelen, A. A simple method for calibration of a scatterometer over the ocean. *J. Atmos. Ocean. Technol.* **1999**, *16*, 275–281. [[CrossRef](#)]
24. Wang, Z.; Stoffelen, A.; Fois, F.; Verhoef, A.; Zhao, C.; Lin, M.; Chen, G. SST dependence of Ku-and C-band backscatter measurements. *IEEE J. Sel. Top. Appl. Earth Obs. Remote Sens.* **2017**, *10*, 2135–2146. [[CrossRef](#)]

Disclaimer/Publisher’s Note: The statements, opinions and data contained in all publications are solely those of the individual author(s) and contributor(s) and not of MDPI and/or the editor(s). MDPI and/or the editor(s) disclaim responsibility for any injury to people or property resulting from any ideas, methods, instructions or products referred to in the content.